Proceedings of the 9th World Congress on Mechanical, Chemical, and Material Engineering (MCM'23)
Brunel University, London, United Kingdom - August 06-08, 2023
Paper No. ICMIE 123
DOI: 10.11159/icmie23.123

Forced Convective Heat Transfer for Stokes Flow with Viscous Dissipation in Wavy Channels

Mohamed Shaimi[1], Rabha Khatyr[2], Jaafar Khalid Naciri[3]
Laboratory of Mechanics, Faculty of Sciences Aïn Chock, Hassan II University of Casablanca
Km 8 Route d'El Jadida, B.P 5366 Maarif 20100, Casablanca 20000, Morocco
[1] mohamed.shaimi-etu@etu.univh2c.ma ; [2] khatyrrabha@gmail.com ; [3] naciriuh2c@gmail.com

Abstract **-** In this paper, an asymptotic solution of the forced convective heat transfer for Stokes flow including viscous dissipation in a two-dimensional sinusoidal wavy channel is presented. The velocity components, pressure, and temperature distributions are sought as an asymptotic expansion in terms of the amplitude to half-mean-height ratio up to the second order. The Nusselt number is calculated in terms of the amplitude to half-mean-height ratio, α, and the half-mean-height to wavelength ratio, ε. In addition to that, a numerical solution, by using ANSYS Fluent solver and integrating Python scripting to automate several parts of the simulations, is presented to validate the asymptotic solution. It is found that the asymptotic and numerical solutions are in good agreement with slight quantitative differences for $\alpha = 0.2$ or $\varepsilon = 0.5$. However, as α increases further, there is a change in the behavior of the Nusselt number defined at the wall due to the use of Taylor series expansions for the boundary conditions which induces an approximated corrugated channel that differ slightly from the exact sinusoidal channel as α increases.

Keywords**:** Forced Convective Heat Transfer, Stokes Flow, Asymptotic Solution, Numerical Solution

1. Introduction

The Stokes flow is the flow for very low Reynolds numbers which is one of the fundamental topics in fluid mechanics that has many applications in various industrial trends such as microfluidics. Analytical perturbations to the well-known Poiseuille flow, which is the laminar flow in long parallel-plate channels or circular pipes are studied by many researchers for different configurations and by using various methods. Wang (1979) [1] and Phan-Thien (1980) [2] presented an asymptotic solution to the Stokes flow respectively in wavy channels and wavy pipes for small amplitudes of the wall corrugation. Later, Vasudeviah and Balamurugan (2001) [3] studied analytically, by using the asymptotic solution for small amplitudes of the wall corrugation, the forced convective heat transfer for Stokes flow in a wavy channel with one surface warmer than the other including viscous dissipation. Wang (2004) [4] and Wang (2006) [5] investigated analytically the Stokes flow respectively through a three-dimensional channel and tube with bumpy walls for small amplitudes of the wall corrugation. Ng and Wang (2010) [6] used the asymptotic solution for the Darcy-Brinkman flow in a wavy channel. Wang (2011) [7] presented the asymptotic solution for the slip flow in wavy channels. Recently, Lei *et al.* (2019) [8] studied the electro-osmotic pumping through a bumpy microtube using the asymptotic solution. Okechi and Asghar (2020) [9] investigated the Darcy-Brinkman flow in a corrugated curved channel.

The objective of this paper is to present an asymptotic solution, similar to those presented in [4,5], of the forced convective heat transfer for Stokes flow in sinusoidal wavy channels including viscous dissipation with a validation by using ANSYS Fluent solver. The asymptotic solution is sought in terms of the small amplitude to half-mean-height ratio up to the second order. The boundary conditions at the walls, no-slip flow and isothermal conditions, are expanded as Taylor series in terms of the small amplitude to the half-mean-height ratio which leads to an approximated corrugated channel. Thus, this paper attempts to validate the correctness of this approximation as well as to investigate its limits and effect on the results' behavior. The numerical solution is obtained by using ANSYS Fluent solver with the integration of Python scripting to automate several parts of the simulations.

This paper is divided into four sections. The second section presents the analysis including the geometrical configuration, mathematical formulation, asymptotic solution, parameter definitions, and numerical solution. The third section presents the results and discussions. Finally, the conclusion is presented with a summary of this work.

2. Analysis

2.1. Geometrical Configuration

The two-dimensional sinusoidal wavy channel is considered infinite. Figure 1 shows one period of the two-dimensional sinusoidal channel. The upper and lower isothermal walls are given respectively by:

$$y_u^*(x^*) = H + a\,sin\left(\frac{2\pi x^*}{L}\right);\quad y_l^*(x^*) = -H - a\,sin\left(\frac{2\pi x^*}{L}\right) \tag{1}$$

where H is half-height of the parallel-plate channel ($a = 0$) which is the half-mean-height, a is the amplitude of the sinusoidal channel, and L is the period of the sinusoidal channel which is the wavelength. (x^*, y^*) are the cartesian coordinates.

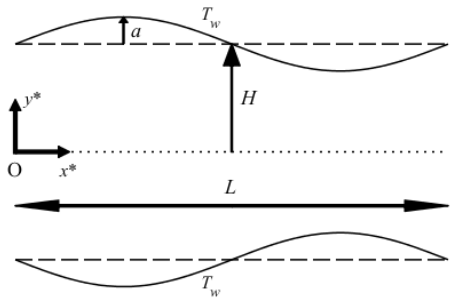

Fig. 1: One period of the two-dimensional sinusoidal channel.

2.2. Mathematical Formulation

The forced convective heat transfer for Stokes flow of Newtonian fluid with constant thermo-physical properties and negligible body forces including viscous dissipation is governed by the following reduced versions of the mass, momentum, and energy conservation equations:

$$\frac{\partial u^*}{\partial x^*} + \frac{\partial \mathrm{v}^*}{\partial y^*} = 0;\quad \frac{\partial^2 u^*}{\partial x^{*2}} + \frac{\partial^2 u^*}{\partial y^{*2}} = \frac{1}{\mu}\frac{\partial p^*}{\partial x^*};\quad \frac{\partial^2 \mathrm{v}^*}{\partial x^{*2}} + \frac{\partial^2 \mathrm{v}^*}{\partial y^{*2}} = \frac{1}{\mu}\frac{\partial p^*}{\partial y^*} \tag{2}$$

$$\frac{\partial^2 T^*}{\partial x^{*2}} + \frac{\partial^2 T^*}{\partial y^{*2}} = -\frac{2\mu}{k}\left[\left(\frac{\partial u^*}{\partial x^*}\right)^2 + \left(\frac{\partial \mathrm{v}^*}{\partial y^*}\right)^2 + \frac{1}{2}\left(\frac{\partial u^*}{\partial y^*} + \frac{\partial \mathrm{v}^*}{\partial x^*}\right)^2\right] \tag{3}$$

where u^* and v^* are the velocity components respectively along x^* and y^*. μ, k, p^*, and T^* are respectively the viscosity, thermal conductivity, pressure, and temperature of the fluid.

The boundary conditions, no-slip and isothermal conditions, at the upper and lower walls are given respectively by:

$$f^*\left(x^*, y^* = y_u^*(x^*)\right) = f^*\left(x^*, y^* = y_l^*(x^*)\right) = 0;\quad T^*\left(x^*, y^* = y_u^*(x^*)\right) = T^*\left(x^*, y^* = y_l^*(x^*)\right) = T_w \tag{4}$$

where T_w is the constant wall temperature and f^* is u^* or v^*.

The sinusoidal channel is periodic with an infinite length. Therefore, only one period is studied and the flow is considered periodic hydrodynamically and thermally fully developed. Thus, the solutions at the inlet and outlet of the studied period are related by the following equations:

$$f^*(x^*, y^*) = f^*(x^* + L, y^*);\quad p^*(x^*, y^*) = p^*(x^* + L, y^*) + \Delta p^* \tag{5}$$

where Δp^* is the pressure drop across one period and f^* is u^*, v*, or T^*.

Defining the following dimensionless variables as:

$$x = \frac{x^*}{L};\quad y = \frac{y^*}{H};\quad u = \frac{u^*}{U};\quad \mathrm{v} = \frac{\mathrm{v}^*}{V};\quad p = \frac{p^*}{P};\quad T = \frac{T^* - T_w}{T_c - T_w} \tag{6}$$

where U, V, P, and T_c are respectively characteristic values of the longitudinal velocity, transversal velocity, pressure, and temperature.

Substituting Eq. (6) into Eqs. (2) and (3) leads to the following dimensionless governing equations:

$$\frac{\partial u}{\partial x} + \frac{\partial \mathrm{v}}{\partial y} = 0;\quad \varepsilon^2\frac{\partial^2 u}{\partial x^2} + \frac{\partial^2 u}{\partial y^2} = \frac{\partial p}{\partial x};\quad \varepsilon^4\frac{\partial^2 \mathrm{v}}{\partial x^2} + \varepsilon^2\frac{\partial^2 \mathrm{v}}{\partial y^2} = \frac{\partial p}{\partial y} \tag{7}$$

$$\varepsilon^2\frac{\partial^2 T}{\partial x^2} + \frac{\partial^2 T}{\partial y^2} = -2Br\left[\varepsilon^2\left(\frac{\partial u}{\partial x}\right)^2 + \varepsilon^2\left(\frac{\partial \mathrm{v}}{\partial y}\right)^2 + \frac{1}{2}\left(\frac{\partial u}{\partial y} + \varepsilon^2\frac{\partial \mathrm{v}}{\partial x}\right)^2\right] \tag{8}$$

where $U = \frac{PH^2}{\mu L}$, $V = \frac{H}{L}U$ from the continuity equation, $Br = \frac{\mu U^2}{k(T_c - T_w)}$ is the Brinkman number that accounts for viscous dissipation, and $\varepsilon = \frac{H}{L}$ is a dimensionless parameter, half-mean-height to wavelength ratio, related to the existence of the transversal velocity.

The dimensionless upper and lower walls are given by:

$$y_u(x) = \frac{y_u^*(x^*)}{H} = 1 + \alpha\, sin(2\pi x);\quad y_l(x) = \frac{y_l^*(x^*)}{H} = -1 - \alpha\, sin(2\pi x) \tag{9}$$

where $\alpha = \frac{a}{H}$ is a dimensionless number, amplitude to half-mean-height ratio, related to the deformation of the parallel-plate channel.

The dimensionless boundary conditions at the walls are given by:

$$f\big(x, y = y_u(x)\big) = f\big(x, y = y_l(x)\big) = 0 \tag{10}$$

where f is u, v, or T.

The dimensionless periodic conditions are given by:

$$f(x, y) = f(x + 1, y);\quad p(x, y) = p(x + 1, y) + \Delta p \tag{11}$$

where $\Delta p = \frac{\Delta p^*}{P}$ is the dimensionless pressure drop across one period and f is u, v, or T.

2.3. Asymptotic Solution

The solutions are sought as an asymptotic expansion in terms of $\alpha \ll 1$ up to the second order as follows:

$$\begin{aligned} &u = u_0 + \alpha u_1 + \alpha^2 u_2 + O(\alpha^3);\quad \mathrm{v} = \mathrm{v}_0 + \alpha \mathrm{v}_1 + \alpha^2 \mathrm{v}_2 + O(\alpha^3);\quad p = p_0 + \alpha p_1 + \alpha^2 p_2 + O(\alpha^3);\\ &T = T_0 + \alpha T_1 + \alpha^2 T_2 + O(\alpha^3) \end{aligned} \tag{12}$$

The boundary conditions at the upper and lower walls are expanded as Taylor series respectively about $y = 1$ and $y = -1$ as follows:

$$f|_{\pm 1 \pm \alpha\, sin(2\pi x)} = f|_{\pm 1} \pm \alpha\, sin(2\pi x)\left.\frac{\partial f}{\partial y}\right|_{\pm 1} + \frac{\alpha^2\left(sin(2\pi x)\right)^2}{2}\left.\frac{\partial^2 f}{\partial y^2}\right|_{\pm 1} + O(\alpha^3) = 0 \tag{13}$$

where f is u, v, or T.

Substituting Eq. (12) into Eq. (13) leads to the following conditions for each order of α:

$$f_0|_{\pm 1} = 0; \quad f_1|_{\pm 1} = \mp\, sin(2\pi x)\left.\frac{\partial f_0}{\partial y}\right|_{\pm 1}; \quad f_2|_{\pm 1} = \mp\, sin(2\pi x)\left.\frac{\partial f_1}{\partial y}\right|_{\pm 1} - \frac{\left(sin(2\pi x)\right)^2}{2}\left.\frac{\partial^2 f_0}{\partial y^2}\right|_{\pm 1} \tag{14}$$

where f is u, v, or T.

The zeroth order, α^0, represents the solution for $\alpha = 0$ which is the case of the parallel-plate channel. Therefore, $\varepsilon \to 0$ due to the unidirectional velocity in the Poiseuille flow. Thus, the known solutions of the Poiseuille flow are given as follows:

$$u_0(y) = 1 - y^2; \quad \mathrm{v}_0 = 0; \quad p_0(x) = -2x; \quad T_0(y) = \frac{Br}{3}(1 - y^4) \tag{15}$$

where $p_0(x = 0) = 0$ is considered at the inlet of the studied period and $\Delta p = 2$ is the dimensionless pressure drop across the period.

The system of equations for the first order, α^1, is given by:

$$\frac{\partial u_1}{\partial x} + \frac{\partial \mathrm{v}_1}{\partial y} = 0; \quad \varepsilon^2\frac{\partial^2 u_1}{\partial x^2} + \frac{\partial^2 u_1}{\partial y^2} = \frac{\partial p_1}{\partial x}; \quad \varepsilon^4\frac{\partial^2 \mathrm{v}_1}{\partial x^2} + \varepsilon^2\frac{\partial^2 \mathrm{v}_1}{\partial y^2} = \frac{\partial p_1}{\partial y} \tag{16}$$

$$\varepsilon^2\frac{\partial^2 T_1}{\partial x^2} + \frac{\partial^2 T_1}{\partial y^2} = -2Br\left[\frac{du_0}{dy}\left(\frac{\partial u_1}{\partial y} + \varepsilon^2\frac{\partial \mathrm{v}_1}{\partial x}\right)\right] \tag{17}$$

After the observation of the governing equations and the boundary conditions, while taking into consideration the periodic conditions, the solutions are sought in the following forms:

$$\begin{aligned} &u_1(x,y) = U_1(y)sin(2\pi x); \quad \mathrm{v}_1(x,y) = V_1(y)cos(2\pi x); \quad p_1(x,y) = P_1(y)cos(2\pi x); \\ &T_1(x,y) = \Theta_1(y)sin(2\pi x) \end{aligned} \tag{18}$$

where U_1, V_1, P_1, and Θ_1 are unknown functions that are determined by using the first-order governing equations with the associated boundary conditions.

The forms in Eq. (18) can be justified explicitly by using the periodic conditions to express u_1, v_1, p_1, and T_1 as Fourier series. Noting that the cosines and sines are orthogonal, equations of each function can be obtained with associated boundary conditions. Finally, all the functions are found to be null except those presented in Eq. (18).

Substituting Eq. (18) into Eqs. (16) and (17) and after some work done by combining the equations to eliminate $U_1(y)$ and $P_1(y)$ from the equation of $V_1(y)$, Eqs. (16) and (17) become:

$$\frac{d^4 V_1}{dy^4} - 8\pi^2\varepsilon^2\frac{d^2 V_1}{dy^2} + 16\pi^4\varepsilon^4 V_1(y) = 0; \quad U_1(y) = \frac{-1}{2\pi}\frac{dV_1}{dy}; \quad P_1(y) = \frac{-1}{2\pi}\frac{d^2 U_1}{dy^2} + 2\pi\varepsilon^2 U_1(y) \tag{19}$$

$$\frac{d^2\Theta_1}{dy^2} - 4\pi^2\varepsilon^2\Theta_1(y) = 4y\, Br\left(\frac{dU_1}{dy} - 2\pi\varepsilon^2 V_1(y)\right) \tag{20}$$

Substituting Eq. (18) into Eq. (14) leads to the following conditions for the first order, α^1:

$$U_1(y=\pm1)=2;\quad V_1(y=\pm1)=0;\quad \Theta_1(y=\pm1)=\frac{4}{3}Br \tag{21}$$

The system of equations for the second order, α^2, is given by:

$$\frac{\partial u_2}{\partial x}+\frac{\partial \mathrm{v}_2}{\partial y}=0;\quad \varepsilon^2\frac{\partial^2 u_2}{\partial x^2}+\frac{\partial^2 u_2}{\partial y^2}=\frac{\partial p_2}{\partial x};\quad \varepsilon^4\frac{\partial^2 \mathrm{v}_2}{\partial x^2}+\varepsilon^2\frac{\partial^2 \mathrm{v}_2}{\partial y^2}=\frac{\partial p_2}{\partial y} \tag{22}$$

$$\varepsilon^2\frac{\partial^2 T_2}{\partial x^2}+\frac{\partial^2 T_2}{\partial y^2}=-2Br\left[\varepsilon^2\left(\frac{\partial u_1}{\partial x}\right)^2+\varepsilon^2\left(\frac{\partial \mathrm{v}_1}{\partial y}\right)^2+\frac{du_0}{dy}\left(\frac{\partial u_2}{\partial y}+\varepsilon^2\frac{\partial \mathrm{v}_2}{\partial x}\right)+\frac{1}{2}\left(\frac{\partial u_1}{\partial y}+\varepsilon^2\frac{\partial \mathrm{v}_1}{\partial x}\right)^2\right] \tag{23}$$

Following a similar procedure to that presented for the first order with the observation of Eqs. (22) and (23) and conditions, (14), the solutions are sought in the following forms:

$$\begin{aligned}&u_2(x,y)=U_{20}(y)+U_{21}(y)cos(4\pi x);\quad \mathrm{v}_2(x,y)=V_2(y)sin(4\pi x);\quad p_2(x,y)=P_2(y)sin(4\pi x);\\&T_2(x,y)=\Theta_{20}(y)+\Theta_{21}(y)cos(4\pi x)\end{aligned} \tag{24}$$

where U_{20}, U_{21}, V_2, P_2, Θ_{20}, and Θ_{21} are unknown functions that are determined by using the second-order governing equations with the associated boundary conditions.

Substituting Eq. (24) into Eqs. (22) and (23) and after some work similar to that presented for the first order, the following equations are obtained:

$$\begin{aligned}&\frac{d^4V_2}{dy^4}-32\pi^2\varepsilon^2\frac{d^2V_2}{dy^2}+256\pi^4\varepsilon^4V_2(y)=0;\quad \frac{d^2U_{20}}{dy^2}=0;\quad U_{21}(y)=\frac{1}{4\pi}\frac{dV_2}{dy};\\&P_2(y)=\frac{1}{4\pi}\frac{d^2U_{21}}{dy^2}+4\pi\varepsilon^2U_{21}(y)\end{aligned} \tag{25}$$

$$\begin{aligned}&\frac{d^2\Theta_{20}}{dy^2}=-2Br\left[2\pi^2\varepsilon^2\big(U_1(y)\big)^2+\frac{1}{2}\varepsilon^2\left(\frac{dV_1}{dy}\right)^2-2y\left(\frac{dU_{20}}{dy}\right)+\frac{1}{4}\left(\frac{dU_1}{dy}\right)^2+\pi^2\varepsilon^4\big(V_1(y)\big)^2-\pi\varepsilon^2V_1(y)\frac{dU_1}{dy}\right];\\&\frac{d^2\Theta_{21}}{dy^2}-16\pi^2\varepsilon^2\Theta_{21}(y)=-2Br\left[2\pi^2\varepsilon^2\big(U_1(y)\big)^2+\frac{1}{2}\varepsilon^2\left(\frac{dV_1}{dy}\right)^2-2y\left(\frac{dU_{21}}{dy}+4\pi\varepsilon^2V_2(y)\right)-\frac{1}{4}\left(\frac{dU_1}{dy}\right)^2\right.\\&\left.-\pi^2\varepsilon^4\big(V_1(y)\big)^2+\pi\varepsilon^2V_1(y)\frac{dU_1}{dy}\right]\end{aligned} \tag{26}$$

Substituting Eq. (24) into Eq. (14) leads to the following conditions for the second order, α^2:

$$\begin{aligned}&U_{20}(y=\pm1)=\frac{1}{2}\mp\frac{1}{2}\frac{dU_1}{dy}\bigg|_{y=\pm1};\quad U_{21}(y=\pm1)=-\frac{1}{2}\pm\frac{1}{2}\frac{dU_1}{dy}\bigg|_{y=\pm1};\quad V_2(y=\pm1)=\mp\frac{1}{2}\frac{dV_1}{dy}\bigg|_{y=\pm1};\\&\Theta_{20}(y=\pm1)=Br\mp\frac{1}{2}\frac{d\Theta_1}{dy}\bigg|_{y=\pm1};\quad \Theta_{21}(y=\pm1)=-Br\pm\frac{1}{2}\frac{d\Theta_1}{dy}\bigg|_{y=\pm1}\end{aligned} \tag{27}$$

Equations (19)-(20) and (25)-(26) are solved consecutively with the help of symbolic computation as well as for the determination of the integration constants by solving Eqs. (21) and (27).

2.4. Parameter Definitions

The dimensionless flow rate and the Nusselt number are defined respectively as follows:

$$Q = \int_{y_l(x)}^{y_u(x)} u(x,y)dy\,; \quad Nu(x) = \frac{-4\left.\frac{\partial T}{\partial n}\right|_{y=y_u(x)}}{T_b(x)} \tag{28}$$

where $\left.\frac{\partial T}{\partial n}\right|_{y=y_u(x)}$ is the normal derivative of the temperature to the upper wall noting that the Nusselt number at the lower wall is the same as at the upper wall due to the symmetry and $T_b(x)$ is the dimensionless bulk temperature. $\left.\frac{\partial T}{\partial n}\right|_{y=y_u(x)}$ and $T_b(x)$ are respectively given by:

$$\left.\frac{\partial T}{\partial n}\right|_{y=y_u(x)} = \frac{-\varepsilon^2\left.\frac{\partial T}{\partial x}\right|_{y=y_u(x)}\frac{dy_u}{dx}}{\sqrt{1+\left(\varepsilon\frac{dy_u}{dx}\right)^2}} + \frac{\left.\frac{\partial T}{\partial y}\right|_{y=y_u(x)}}{\sqrt{1+\left(\varepsilon\frac{dy_u}{dx}\right)^2}}; \quad T_b(x) = \frac{\int_{y_l(x)}^{y_u(x)} u(x,y)\,T(x,y)dy}{\int_{y_l(x)}^{y_u(x)} u(x,y)dy} \tag{29}$$

The derivatives and the integrations of the temperature in Eq. (28) are expanded as Taylor series up to the second order of α:

$$\left.\frac{\partial T}{\partial y}\right|_{y=1+\alpha\,sin(2\pi x)} = \left.\frac{\partial T}{\partial y}\right|_{y=1} + \alpha\,sin(2\pi x)\left.\frac{\partial^2 T}{\partial y^2}\right|_{y=1} + \frac{\alpha^2\left(sin(2\pi x)\right)^2}{2}\left.\frac{\partial^3 T}{\partial y^3}\right|_{y=1} + O(\alpha^3);$$
$$\left.\frac{\partial T}{\partial x}\right|_{y=1+\alpha\,sin(2\pi x)}\frac{dy_u}{dx} = 2\pi\alpha\,cos(2\pi x)\left(\left.\frac{\partial T}{\partial x}\right|_{y=1} + \alpha\,sin(2\pi x)\left.\frac{\partial^2 T}{\partial y\partial x}\right|_{y=1}\right) + O(\alpha^3) \tag{30}$$

$$\int_{-1-\alpha\,sin(2\pi x)}^{1+\alpha\,sin(2\pi x)} f(x,y)dy = \int_{-1}^{1} f(x,y)dy + \alpha\,sin(2\pi x)\big(f(x,y=1)+f(x,y=-1)\big)$$
$$+\frac{\alpha^2\left(sin(2\pi x)\right)^2}{2}\left(\left.\frac{\partial f}{\partial y}\right|_{y=1} - \left.\frac{\partial f}{\partial y}\right|_{y=-1}\right) + O(\alpha^3) \tag{31}$$

where $f(x,y)$ is $u(x,y)$ or $u(x,y)\,T(x,y)$ and Eq. (12) is substituted into Eqs. (30) and (31) then only terms up to α^2 remain.

The dimensionless flow rate and the Nusselt number are calculated with the help of symbolic computation. For the parallel-plate channel ($\alpha = 0$), $Nu = 17.5$ which is the known value of the fully developed Nusselt number with viscous dissipation [10]. The dimensionless flow rate, after the calculations with the help of symbolic computation, is found as $Q(\alpha,\varepsilon) = \frac{4}{3} + \alpha^2 Q_2(\varepsilon) + O(\alpha^3)$ where $Q_2(\varepsilon) = \int_{-1}^{1} u_2(x,y)dy - 2\left(sin(2\pi x)\right)^2$. It is verified that Q is constant with negligible quantitative fluctuations.

2.5. Numerical Solution

The numerical solution is obtained by using ANSYS Fluent solver. Python scripting is used to create the geometry and automate several parts of the simulations [11,12]. The element size used to create the structured mesh in this paper

is $0.02H$. The convergence criterion used in this study is 10^{-6} for the continuity and momentum conservation equations and 10^{-12} for the energy equation to get accurate results. Table 1 shows the grid independence test performed for three different sinusoidal channels ($\varepsilon = 0.1;\ \alpha = 0.1, \varepsilon = 0.1;\ \alpha = 0.2, \varepsilon = 0.5;\ \alpha = 0.1$). The mean square of the relative difference for 11 local points equally distanced, x_i, of Nu, $E = \sqrt{\frac{1}{11}\sum_{i=1}^{11}\left|\frac{Nu(x_i)-Nu_e(x_i)}{Nu(x_i)}\cdot 100\right|^2}$, is used to evaluate the changes of Nu in % as the element size changes, Nu_e. The results show that the chosen element size gives a very good precision needed to validate the asymptotic solution.

Table 1: Grid independence test.

Element size$/_H$		0.2	0.1	0.04	0.02
E	$\varepsilon = 0.1;\ \alpha = 0.1$	5.294	1.402	0.180	----
	$\varepsilon = 0.1;\ \alpha = 0.2$	4.885	1.243	0.223	----
	$\varepsilon = 0.5;\ \alpha = 0.1$	5.895	1.372	0.186	----

3. Results and Discussions

Figures 2(a)-(c) show the evolution of the Nusselt number, Nu, as a function of the dimensionless longitudinal coordinate, x, for $\varepsilon = 0.1;\ \alpha = 0.1$, $\varepsilon = 0.1;\ \alpha = 0.2$, and $\varepsilon = 0.5;\ \alpha = 0.1$ with a comparison between the asymptotic solution and numerical solution. Figures 2(a)-(c) show that the asymptotic and numerical solutions are in good agreement for $\varepsilon = 0.1;\ \alpha = 0.1$ but as ε increases, quantitative differences are observed. Furthermore, as α increases, there are quantitative differences observed in addition to a change in the behavior of Nu found by using the asymptotic solution. This is due to the use of Taylor series expansion of the boundary conditions at the walls. Therefore, the presented asymptotic solution is a solution for an approximated corrugated channel that is close to the exact sinusoidal channel for small α while it differs slightly as α increases.

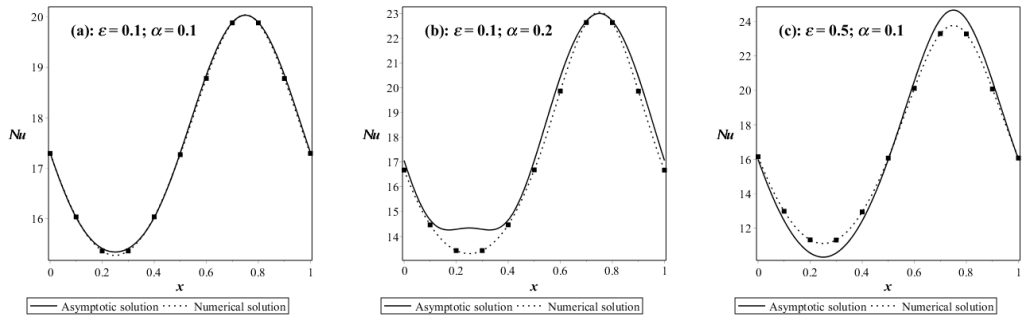

Fig. 2: Evolution of the Nusselt number as a function of x with a comparison between asymptotic and numerical solutions.

Table 2 shows that the asymptotic and numerical solutions of Q are in good agreement with very small quantitative differences for $\alpha = 0.2$ or $\varepsilon = 0.5$. As can be seen from Figs. 2(a)-(c) and Table 2 the Nusselt number is more sensitive to the differences between the exact and approximated channel which leads to the change in behavior observed in Fig. 2(b) since Nusselt number is defined as the derivative of the temperature at the wall as opposed to the dimensionless flow rate which is defined as an integral over an area of a section.

Table 2: Comparison between asymptotic and numerical solutions of the dimensionless flow rate, Q.

	$\varepsilon = 0.1;\ \alpha = 0.1$	$\varepsilon = 0.1;\ \alpha = 0.2$	$\varepsilon = 0.5;\ \alpha = 0.1$
Q (Numerical solution)	1.287	1.167	1.231
Q (Analytical solution)	1.290	1.161	1.225

4. Conclusion

A comparison between an asymptotic and numerical solution to the forced convective heat transfer for Stokes flow viscous dissipation in a two-dimensional sinusoidal channel is presented in this paper. The asymptotic solution is sought an expansion in terms of the amplitude to half-mean-height ratio up to the second order and determined with the help of symbolic computation while the numerical solution is obtained by using ANSYS Fluent solver with the integration of scripting to automate several parts of the simulations. It is found that the asymptotic and numerical solutions are in good agreement with small quantitative differences as the amplitude to half-mean-height ratio or half-mean-height to wavelength ratio increases ($\alpha = 0.2$ or $\varepsilon = 0.5$) noting that as the amplitude to half-mean-height ratio increases a change in the behavior of the Nusselt number is observed due to its definition at the approximated wall induced from the Taylor series expansions of the boundary conditions. To get more accurate results for the higher amplitude to half-mean-height ratios, higher orders can be included in the asymptotic solution. The presented asymptotic solution can be used in the case of three-dimensional ducts, curved pipes, slip flows, porous mediums, and many more which has several practical applications in various industrial trends to get analytical solutions that are less time-consuming compared to Computational Fluid Dynamics simulations.

Acknowledgements

This work is done with the financial support of the National Center for Scientific and Technical Research (CNRST).

References

[1] C. Y. Wang, "On Stokes flow between corrugated plates," *J. Appl. Mech*., vol. 46, no. 2, pp. 462-464, 1979. https://doi.org/10.1115/1.3424575

[2] N. Phan-Thien, "On the Stokes flow of viscous fluids through corrugated pipes," *J. Appl. Mech*., vol. 47, no. 4, pp. 961-963, 1980. https://doi.org/10.1115/1.3153825

[3] M. Vasudeviah and K. Balamurugan, "On forced convective heat transfer for a stokes flow in a wavy channel," *Int. Commun. Heat Mass Transfer*, vol. 28, no. 2, pp. 289-297, 2001. https://doi.org/10.1016/S0735-1933(01)00235-4

[4] C. Y. Wang, "Stokes flow through a channel with three-dimensional bumpy walls," *Phys. Fluids*, vol. 16, no. 6, pp. 2136-2139, 2004. https://doi.org/10.1063/1.1707023

[5] C. Y. Wang, "Stokes flow through a tube with bumpy wall," *Phys. Fluids*, vol. 18, 078101, 2006. https://doi.org/10.1063/1.2214883

[6] C. O. Ng and C. Y. Wang, "Darcy-Brinkman flow through a corrugated channel," *Transp. Porous Media*, vol. 85, pp. 605-618, 2010. https://doi.org/10.1007/s11242-010-9580-1

[7] C. Y. Wang, "On Stokes slip flow through a transversely wavy channel," *Mech. Res. Commun*., vol. 38, no. 3, pp. 249-254, 2011. https://doi.org/10.1016/j.mechrescom.2011.02.006

[8] J. C. Lei, C. C. Chang, and C. Y. Wang, "Electro-osmotic pumping through a bumpy microtube: Boundary perturbation and detection of roughness," *Phys. Fluids*, vol. 31, 012001, 2019. https://doi.org/10.1063/1.5063869

[9] N. F. Okechi and S. Asghar, "Darcy-Brinkman flow in a corrugated curved channel," *Transp. Porous Media*, vol. 135, pp. 271-286, 2020. https://doi.org/10.1007/s11242-020-01473-2

[10] R. K. Shah and A. L. London, *Laminar flow forced convection in ducts*. Academic Press, New York, 1978.

[11] M. Shaimi, R. Khatyr, and J. Khalid Naciri, "Ansys Fluent automation for fluid flow and heat transfer in corrugated channels," in *Proceedings of the International Conference on Fluid Flow, Heat and Mass Transfer*, Niagara Falls, Canada, 2022, vol. 9, 206. https://doi.org/10.11159/ffhmt22.206

[12] M. Shaimi, R. Khatyr, and J. Khalid Naciri, "Ansys Mechanical automation using Python for the steady state thermal analysis of fins," in *Proceedings of the World Congress on Mechanical, Chemical, and Material Engineering*, Prague, Czech Republic, 2022, vol. 8, HTFF 178. https://doi.org/10.11159/htff22.178